Materials Today Bio 26 (2024) 101038

Contents lists available at ScienceDirect

Materials Today Bio

journal homepage: www.journals.elsevier.com/materials-today-bio

Preliminary study of the homeostatic regulation of osseointegration by nanotube topology

Tao Chen [a,b,c], MingXing Ren [a,b,c], YuZhou Li [a,b,c], Zheng Jing [a,b,c], XinXin Xu [a,b,c], FengYi Liu [a,b,c], DingQiang Mo [a,b,c], WenXue Zhang [a,b,c], Jie Zeng [a,b,c], He Zhang [a,b,c,**], Ping Ji [a,b,c,***], Sheng Yang [a,b,c,*]

[a] College of Stomatology, Chongqing Medical University, PR China
[b] Chongqing Key Laboratory of Oral Diseases, PR China
[c] Chongqing Municipal Key Laboratory of Oral Biomedical Engineering of Higher Education, PR China

ARTICLE INFO

Keywords:
FAK
PYK2
Osteoclasts
Osteoblasts
Bone homeostasis

ABSTRACT

The ideal implant surface plays a substantial role in maintaining bone homeostasis by simultaneously promoting osteoblast differentiation and limiting overactive osteoclast activity to a certain extent, which leads to satisfactory dynamic osseointegration. However, the rational search for implant materials with an ideal surface structure is challenging and a hot research topic in the field of tissue engineering. In this study, we constructed titanium dioxide titanium nanotubes (TNTs) by anodic oxidation and found that this structure significantly promoted osteoblast differentiation and inhibited osteoclast formation and function while simultaneously inhibiting the total protein levels of proline-rich tyrosine kinase 2 (PYK2) and focal adhesion kinase (FAK). Knockdown of the PYK2 gene by siRNA significantly suppressed the number and osteoclastic differentiation activity of mouse bone marrow mononuclear cells (BMMs), while overexpression of PYK2 inhibited osteogenesis and increased osteoclastic activity. Surprisingly, we found for the first time that neither knockdown nor overexpression of the FAK gene alone caused changes in osteogenesis or osteoclastic function. More importantly, compared with deletion or overexpression of PYK2/FAK alone, coexpression or cosilencing of the two kinases accelerated the effects of TNTs on osteoclastic and osteogenic differentiation on the surface of cells. Furthermore, in vivo experiments revealed a significant increase in positiveexpression-PYK2 cells on the surface of TNTs, but no significant change in positiveexpression -FAK cells was observed. In summary, PYK2 is a key effector molecule by which osteoblasts sense nanotopological mechanical signals and maintain bone homeostasis around implants. These results provide a referable molecular mechanism for the future development and design of homeostasis-based regulatory implant biomaterials.

1. Introduction

Peri-implant bone remodeling occurs via a continuous and complex cycle [1,2].During this process, the dynamic balance between osteoblasts and osteoclasts [3]serves as a key factor in maintaining normal bone volume around the implant [4]. An imbalance between osteoblasts and osteoclasts disrupts the bone structure and affects the stability of the implant [5], which eventually leads to implant loss [6]. Studies have shown that most postimplant failures derive from the suppression of osteoblast function and overactivity of osteoclasts on the implant surface [7]. Therefore, dedicate control of the ratio between bone formation and resorption, ensuring a constant bone volume and maintaining bone homeostasis [8], via optimization of the biological properties of the implant is highly desirable [9].

Surface micro/nanomorphology is a key factor that influences the biological performance of implants [10]. In the early stages after implant placement, surface morphology-mediated biophysical signals are transmitted to adherent cells and thus stimulate signaling cascades that regulate cell biological behaviors [11], including cell migration [12], proliferation [13], and differentiation [14]. In our previous study,

* College of Stomatology, Chongqing Medical University, PR China.
** Corresponding author. College of Stomatology, Chongqing Medical University, PR China.
*** Corresponding author. Chongqing Key Laboratory of Oral Diseases, PR China.
E-mail addresses: kqzhanghe@hospital.cqmu.edu.cn (H. Zhang), jiping@hospital.cqmu.edu.cn (P. Ji), 500283@cqmu.edu.cn (S. Yang).

https://doi.org/10.1016/j.mtbio.2024.101038
Received 27 December 2023; Received in revised form 14 March 2024; Accepted 22 March 2024
Available online 4 April 2024

we found that titanium nanotubes induce dramatic differences in osteocyte fate according to their nanoscale morphology by regulating the adhesion-related FAK/RhoA pathway [15]. By reducing the expression of lamin A/C, titanium nanotubes inhibited the activity of the actin-regulated MRTF-A-SRF complex, thereby reducing the inflammatory response, indicating that titanium nanotubes have good bone immunomodulatory effects and can promote bone integration [16]. Moreover, other groups have reported the inhibitory effect of titanium nanoporous structures (NSs) on osteoclast formation [17]. However, the underlying mechanism remains unclear and controversial. Thus, further exploration of the specific role of titanium NSs in regulating osteocyte fate is needed [18].

Notably, two adherent spot kinases [19], focal adhesive patch kinase (FAK) and proline-rich tyrosine kinase 2 (PYK2), both of which are primary signaling proteins for the intracellular sensing of adhesion signals [20,21], play key roles in mediating the differentiation fate of osteoblastic-osteoclastic cells upon mechanical signaling [22]. In osteoblasts, FAK was previously reported to be a central link in the mechanical induction of osteogenic differentiation and to directly mediate gene regulation [23]. High FAK expression was observed on nanogratings and nanofiber scaffolds [24], which were experimentally validated to act as pro-osteogenic NSs. In contrast, PYK2 was reported to indirectly regulate stem cell migration [25] and osteogenic differentiation [26], affecting the osseointegration process [27]. In osteoclasts, PYK2 was enriched in the footbody proteins of the osteoclast actin ring and colocalized with the adhesion patch protein vinculin, suggesting that PYK2 is an important regulator of osteoclast formation [2]. Severely impaired bone resorption function was observed in PYK2-deficient osteoblasts, and PYK2 contributes to the formation of the osteoblast pedicle structure as well as microtubule stability [28]. Furthermore, in vivo studies revealed that inhibition of PYK2 activity stimulated osteogenesis, suggesting that PYK2 may be a negative regulator of osteogenesis [2]. However, the function of PYK2 in titanium NSs-induced bone formation is unknown. Meanwhile, the expression and function of FAK in titanium NSs-induced osteoclastogenesis have not been fully investigated. Given the importance of adherent spot kinases in osteoblast and osteoclast formation, it is indispensable to clarify the roles of FAK and PYK2 [26] in the regulation of bone homeostasis by titanium NSs.

In this study, we synthesized titanium nanotubes torphology as titanium NSs to discover the effect of osseointegration. We found that titanium NSs play an important role in maintaining bone homeostasis. Moreover, we observed that the expression levels of FAK and PYK2 in MC3T3-E1 cells and bone marrow mononuclear cells (BMMs) were strongly decreased by stimulation with flat Ti. The expression levels of FAK and PYK2 were manipulated by constructing siRNA and with an lentvirus to observe the consequent biological phenotypes of the MC3T3-E1 cells and BMMs. The single knockdown of PYK2, but not FAK, rescued osteogenic function and inhibited osteoclastic activity. PYK2/FAK coexpression and cosilencing further accelerated the effect of the TNTs on osteoclastic differentiation and osteogenic differentiation of cells. In vivo experiments demonstrated a significant increase in positiveexpression-PYK2 cell numbers around the titanium nanoporous implants, while no significant difference in positiveexpression-FAK cells was observed. With these findings, we have identified the unique functional roles of PYK2 and FAK in the responses of osteoblasts and osteoclasts to titanium nanotopography, providing candidate targets for the development of bone-regenerative materials.

2. Materials and methods

2.1. TNT fabrication

TNTs with a diameter of 150 nm were prepared with commercial pure Ti discs (purity: 99.9%, diameter: 34 or 14 mm, thickness: 1 mm, Baoji Titanium Industry, China). A method published in previous studies was followed. Specifically, the flat Ti discs were polished using 320–2000 grit SiC abrasive paper (Electron Microscopy Sciences). Then, the Ti discs were sequentially sonicated in 100% acetone, 70% ethanol, and distilled water for 15 min each before anodization, and the samples were dried in air. Next, Ti discs, acting as an anode, and platinum foil (Alfa Aesar), acting as a cathode, were connected in an electrochemical reaction flask, and 30 V DC power was supplied (Thermo Electron). A glycerol-based electrolyte was prepared with 0.25 wt% ammonium fluoride (Alfa Aesar, 96%) and 2 wt% deionized water. After anodization, the samples were thoroughly washed with deionized water and dried at 80 °C. Finally, a muffle furnace (Thermolyne 6000) was utilized to anneal the samples at 500 °C for 3 h. The nonanodized pure Ti foils (flat Ti) underwent the same treatment except that a voltage of 0 V were applied to the control group. Prior to cell culture experiments, all the experimental samples were sterilized with 70% ethanol for 10–12 h followed by exposure to UV light overnight.

2.2. Cell morphology and EDS

SEM (Hitachi S-4700) was utilized to observe the surface topography of the materials and cell adhesion. The scanning electron microscope equipped with an energy dispersive X-ray spectrometer was also used to analyze calcium nodules that formed by the osteogenic differentiation of MC3T3-E1.

2.3. Cell culture

MC3T3-E1 cells (ATCC) were incubated in alpha-minimum essential medium (αMEM) (Gibco) supplemented with 10% fetal bovine serum (FBS, Gibco) and 1% penicillin–streptomycin (Gibco) at 37 °C in a 5% CO2 environment. To observe the effects of TNTs on cell behavior, MC3T3-E1 cells were seeded onto Flat Ti (control) and TNT substrates, which were placed within polystyrene culture plates. MC3T3-E1 cells (passages 3 to 10) were cultured on FlatTi and TNTs at a density of 500 cells per cm2 for SEM and immunofluorescence staining; 2.5×10^4 cells per cm2 were seeded for all other experiments unless otherwise specified.

2.4. Osteoclast differentiation

Bone marrow cells were obtained from the femurs of WT C57BL/6J mice aged 4–6 weeks and cultured overnight in α-MEM supplemented with 10% FBS (Gibco, USA) and 1% penicillin−streptomycin (Solarbio, China) in a humidified atmosphere of 5% CO2 at 37 °C. The cell suspensions were extracted the next day for gradient centrifugation at 410*g*, and to induce osteoclast formation, bone marrow-derived macrophages (BMMs) were cultured in complete medium containing 44 ng/ml recombinant soluble mouse M-CSF (NovoProtein, China) and 100 ng/ml recombinant soluble mouse RANKL (NovoProtein, China). The effect of OC differentiation was observed by TRAP staining. The cells were fixed by soaking in 4% paraformaldehyde for 20 min and then stained with TRAP (Solarbio, China). The cells with multiple nuclei (nuclei >3) that were TRAP positive were counted as OCs under a light microscope. To verify its function in OCs, osteoclast formation was induced on 96-well bone plates by a bone resorption activity assay, and the depth of bone pits on the bone surface was measured by actin staining. TRAP staining was performed using an acid phosphatase leukocyte kit (Sigma). The sample was mounted on a coverglass and imaged with an optical microscope (Olympus).

2.5. Gene expression analysis

Real-time fluorescence quantitative PCR was used to analyze the expression levels of osteogenic and osteoclastic genes. Total cellular RNA was isolated with TRIzol reagent (Takara, Japan) and reverse-transcribed into cDNA using Prime-Script Master Mix (Takara, Japan).

Real-time quantitative PCR was performed using TB Green Premix Ex *Taq*II (Takara, Japan) and a CFX96 Real-Time PCR detection system (Bio-Rad, USA). Glycerol-dehydrogen-3-phosphate dehydrogenase (GAPDH) was used as the reference gene. The target gene-specific primers specific for Osx, Runx2, Ocn, Bsp, Trap, Nfatc-1, c-Fos, Mmp-9 andRank and Col1 are listed in Table S1.

2.6. Osteogenic differentiation analysis

ALP staining and ALP activity assays were performed in MC3T3-E1 cells cultured on TNT substrates and in the control group Flat Ti) for 7 days. The cells used to detect ALP activity were rinsed with PBS twice and lysed on ice using RIPA lysis buffer for 25 min. The lysates were then collected, centrifuged at 10,000 rpm for 5 min at 4 °C and analyzed with an ALP activity kit (Beyotime Biotechnology) according to the manufacturer's instructions (n = 3). For ALP staining, the cells were rinsed with PBS, fixed with 4% PFA for 10 min and rinsed with DPBS three times. The cells were then stained with reagents from an ALP Staining Kit (Beyotime Biotechnology) according to the manufacturer's instructions (n = 3). Alizarin red staining was measured after 14 or 28 days of culture, and all groups of MC3T3-E1 cells were rinsed with PBS twice, fixed in 4% PFA for 10 min and rinsed with PBS three times. The cells were stained with Alizarin red S (Solarbio) at 37 °C for 30 min and imaged through an optical microscope (Leica) after rinsing with PBS three times.

2.7. Western blotting

The expression of FAK, phosphorylated FAK, PYK2 and phosphorylated PYK2 was examined by Western blotting. After culture for 3 days, RIPA buffer (Thermo Scientific) was used to isolate the total protein from MC3T3-E1 cells and BMMs seeded on the flat Ti and TNT substrates. Analysis buffer was used to dilute the proteins to equalize the concentration, and then the proteins were fractionated by electrophoresis in 10% polyacrylamide gels. All proteins were electrotransferred to PVDF membranes and probed with anti-FAK, anti-pFAK, anti-PYK2, anti-pPYK2, anti-OCN, anti-OPN, and anti-TRAP antibodies at 1:1000. After reaction with a secondary antibody at 1:5000 (HRP-conjugated IgG), ECL (Thermo Scientific) was used to generate chemiluminescence signals from the immunoreactive bands. Finally, ImageJ software was used to analyze the band density in triplicate. GAPDH (Cell Signaling) was chosen as the reference. All primary and secondary antibodies used for Western blotting are listed in Table S3.

2.8. Immunofluorescence staining

The cells were fixed in 4% paraformaldehyde (Sigma) for 10 min and permeabilized with 0.1% Triton X-100 (Sigma) for 5 min. Next, the cells were incubated with primary antibodies (against PYK2, FAK, and TRAP) at a ratio of 1:200 overnight at 4 °C and then with an Alexa Fluor-coupled secondary antibody (1:300) for 1 h and finally with DAPI, (1:1000). F-actin was labeled using Alexa Fluor 488-coupled phalloidin, and PYK2, FAK, and TRAP were labeled using Alexa Fluor 647-coupled DNase-I. Staining was imaged by laser scanning confocal microscopy (LSCM, Germany) to obtain immunofluorescence images, and all primary and secondary antibodies applied to the immunocultures are listed in Table S3.

2.9. Transfection

For lentiviral infection, MC3T3-E1 was inoculated into a 24-well plate and cultured in medium until the cells reached 50% confluent. The cells were then incubated with lentiviral particles (MOI = 20) in a medium supplemented with 5 μg/ml polystyrene. After incubating at 37 °C for 24 h, replace the medium. Stable transduction cells were selected with 5 μg/ml purinomycin and maintained in medium containing 2 μg/ml purinomycin. Real-time fluorescence quantitative PCR was used to verify the effectiveness of lentivirus infection. When BMMs were inoculated in a 6-well plate, the cell density was about 50% the next day. The MOI of lentivirus was 10. After 48 h, the transfection efficiency of the lentivirus was detected by Western blot. For FAK and PYK2 knockdown, MC3T3-E1 cells and BMMs were transfected with siRNA using PepMute siRNA transfection reagent (Signa Gen, USA). The efficiency of the overexpression or knockdown of the target genes was verified by Western blotting or RT-PCR experiments.

2.10. Animal experiment

All animal experiments were performed according to the guidelines of the Animal Care and Use Committee of China and were approved by the ethics committee of Chongqing Medical University Affiliated Hospital of Stomatology (Ethics No. CQHS-REC-2022 (LSNo.164)). SD rats (male, 250–300 g) were divided into two groups: the flat Ti and TNT groups (5 rats per group). After intraperitoneal injection of 5% chloral hydrate (0.7 ml/100 g) for anesthesia, the distal femur of each rat was surgically exposed, and a prepared Ti rod or TNT rod (diameter of 1 mm, length of 10 mm, Baoji Titanium Industry, China) was implanted and sutured with 6–0-filament braided thread in layers. On the 4th, 7th and 14th days after surgery, the rats were killed by CO_2 hypoxia.

2.11. Osteogenic elevation in vivo

Scanning was performed using micro-CT (vivaCT80, SCANCO Medical AG, Switzerland). A ring with a radius of 300 μm around the implant was defined as the region of interest (ROI). 3D images, BV/TV ratios and Tb.Th values were calculated. SCANCO VivaCT40 micro-CT software was used for the analysis. Then, the samples were fixed in 4% paraformaldehyde and decalcified with Na-EDTA (Servicebio, China) for 40 days. The Ti rods and TNT rods were removed from the femur, and the femur was subsequently embedded in paraffin and cut into 7 μm thick sections.

2.12. Immunohistochemistry

Immunohistochemical staining for FAK, PYK2, OCN and OPN was performed. Immunohistochemical analysis: The expression of FAK, PYK2, OCN and OPN in the bone tissue around the implants was detected by immunohistochemistry (IHC) with a primary antibody (1:100 dilution). Briefly, sections were dewaxed with xylene, followed by gradient hydration and antigen recovery with hyaluronidase at 37 °C for 1 h and pepsin at room temperature for 25 min. The sections were then blocked with a secondary antibody containing homologous serum for 30 min. Next, the paraffin sections were incubated with primary antibody at 4 °C. After 12 h, the slices were rinsed with PBS and incubated with secondary antibodies at room temperature for 30 min. A DAB horseradish peroxidase chromogenic kit (Beyotime, Shanghai, China) was used to induce chromogenic reactions.

3. Results

Schematic showing how titanium dioxide nanotube topography affects bone homeostasis by regulating the expression of FAK/PYK2.

3.1. TNTs induced the osteogenic differentiation of MC3T3-E1 cells and altered the expression of FAK and PYK2

Schematic diagram shows that MC3T3-E1 cells were inoculated with Ti nanotube morphology, and the osteogenic differentiation of the cells was promoted under the morphology (Fig. 1A). We synthesized titanium dioxide nanotubes using electrochemical anodic oxidation and examined the morphology of the titanium dioxide nanotubes and smooth

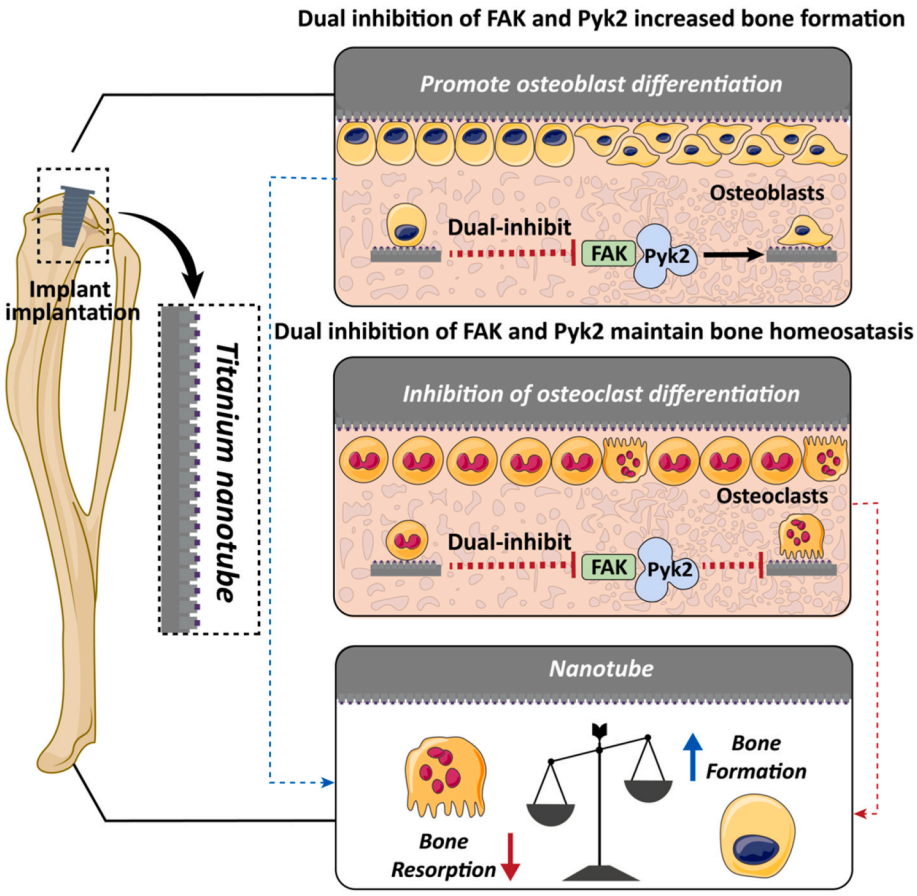

titanium surfaces by SEM (Fig. 1B). Compared with the smooth pure titanium surface, the nanotube surface showed a regular tubular structure, and the wall thickness of the nanotubes was 30 nm, with an inner diameter of 90 nm. To investigate the role of nanotube morphology in the osteogenic differentiation of the cells, the extracellular matrix composition and nodule formation of MC3T3-E1 cells on both the Flat Ti surface and the TNT surface were observed using energy dispersive X-ray (EDX) analysis (Fig. 1C). Spectroscopic analysis revealed that the nodules were calcium-rich minerals formed by the deposition of pan-calcium in the cytoplasm, and irregularly shaped nodules were observed on the TNTs after 21 days of incubation. Real-time PCR revealed that, compared with their expression in MC3T3-E1 cells adhered to flat Ti, after 14 and 21 days of incubation, MC3T3-E1 cells adhered to TNTs expressed significantly increased levels of the following osteogenesis-related genes (Fig. 1D): osteocalcin (Ocn), bone salivary protein (Bsp), RUNT-associated transcription factor 2 (Runx2), and osterix (Osx). After 7 d of culture, alkaline phosphatase (ALP) staining (Fig. S1A) and ALP activity assays showed that the ALP activity in the TNT group was higher than that in the Flat Ti group (Fig. S1C). Alizarin red staining staining (Fig. S1B) and quantitative analysis further showed that the mineralization capacity of the TNT group was significantly better than that of the Flat Ti group after 14 days of culture (Fig. S1D). To further investigate the mechanism by which nanomorphology changes cell fate, we investigated cell morphology. We seeded MC3T3-E1 cells on titanium dioxide nanotubes and smooth titanium surfaces and observed the mucosal pattern of the cells. MC3T3-E1 cells attached to Flat Ti formed wide lamellar feet at the leading edges (Fig. S2), whereas those attached to TNTs formed typical filamentous feet. Moreover, immunofluorescence staining revealed that FAs were bright green dots distributed around the nucleus and at the edges of diffusing cells on Flat Ti (Fig. 1E). Few obvious FAs were observed in the small spindle-shaped cells on the TNTs. We further demonstrated the total FAK and PYK2 protein levels and their phosphorylation levels by Western blotting (Fig. 1F), which showed that the expression of total FAK, pY397-FAK, PYK2, and pY402-PYK2 was impaired by TNT, whereas their levels were significantly elevated on Flat Ti. Collectively, these data suggest that compared with Flat Ti, TNTs inhibit the protein expression of FAK and PYK2 in MC3T3-E1 cells to promote osteogenesis.

3.2. *TNTs inhibited the osteoclastic differentiation of mouse BMMs and altered the expression of FAK and PYK2*

Bone formation is dependent on both osteoblasts and osteoclasts. Next, we further explored the role of nanotopographical surfaces in the osteoclastic differentiation of monocyte macrophages. The schema shows that BMMs cells were inoculated with Ti nanotube morphology, and the osteoclastic differentiation of the cells was inhibited under the morphology (Fig. 2A). We utilized RANKL and M-CSF stimulation on the surface of Flat Ti and TNTs, respectively, to induce the osteoclastic differentiation of BMMs. TRAP immunofluorescence staining and F-actin rings showed that BMMs formed osteoclasts (with >3 nuclei) on the surface of Flat Ti on the fifth day under combined induction with RANKL and M-CSF, in contrast to the surface of TNTs, where almost no osteoclasts formed (Fig. 2B). Real-time PCR revealed that compared with Flat Ti, TNTs significantly inhibited the expression of the osteoclast-related genes Trap, Rank, Ctsk, Mmp-9, c-Fos, and Nfatc-1 compared with that on flat Ti(Fig. 2C). Consistent with these findings, the Western blotting results showed that TRAP expression was significantly inhibited by TNTs (Fig. 2D). To further investigate the mechanism by which nanotopography affects the fate of osteoclasts, we analyzed the expression of FAK and PYK2 in osteoclasts using immunofluorescence staining and found that FAK and PYK2 were also suppressed on the

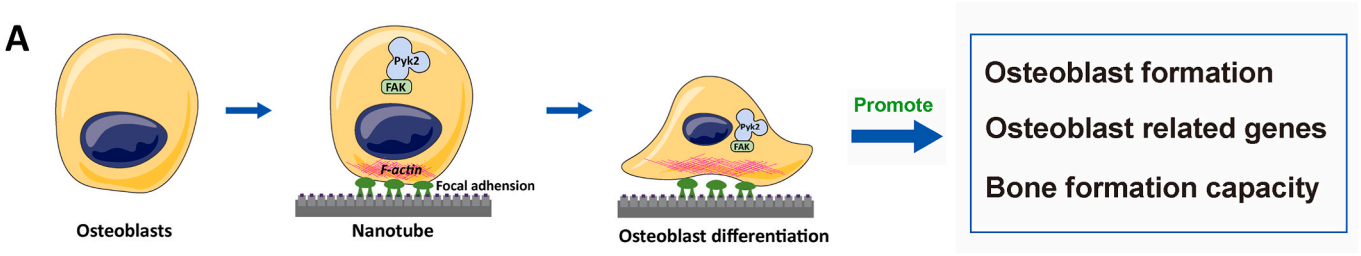

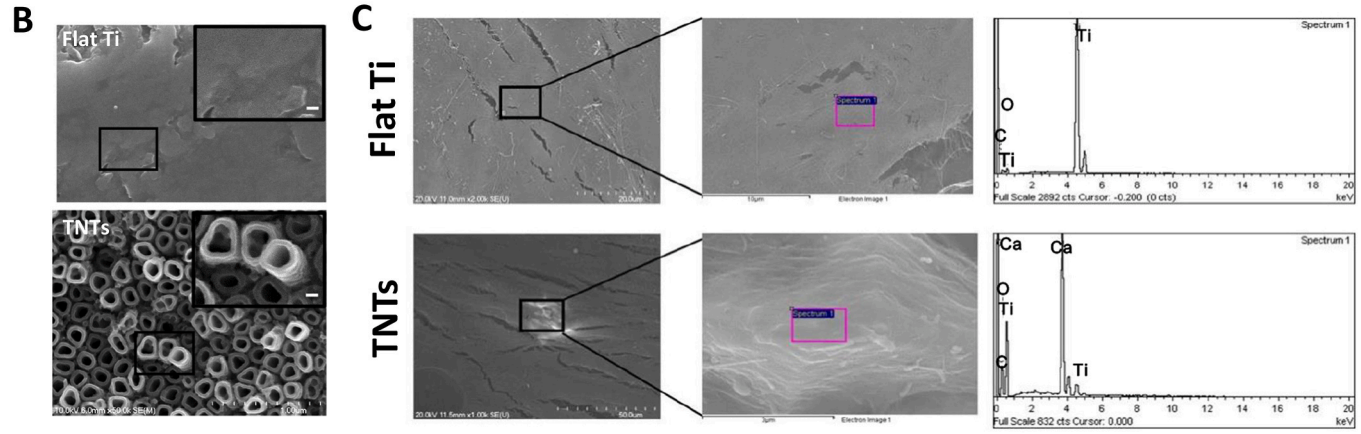

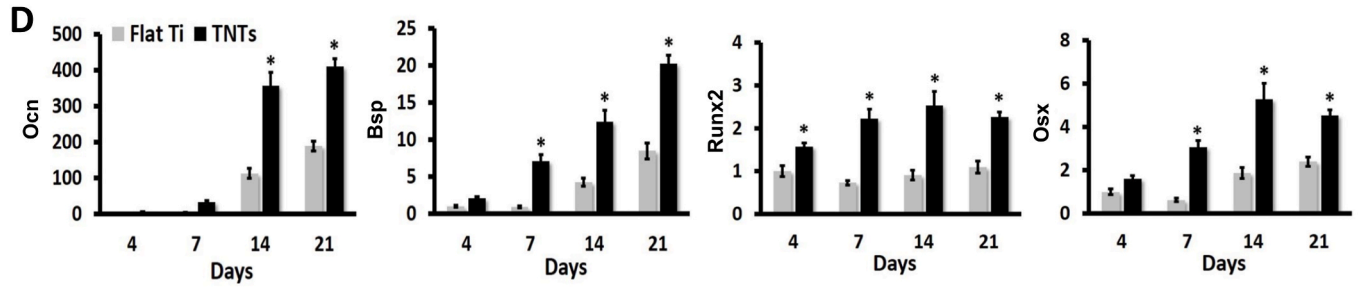

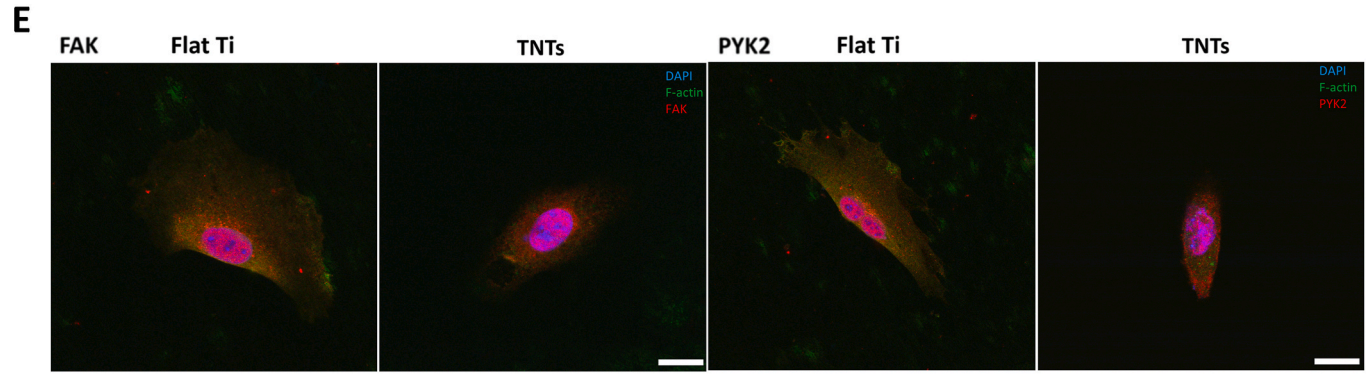

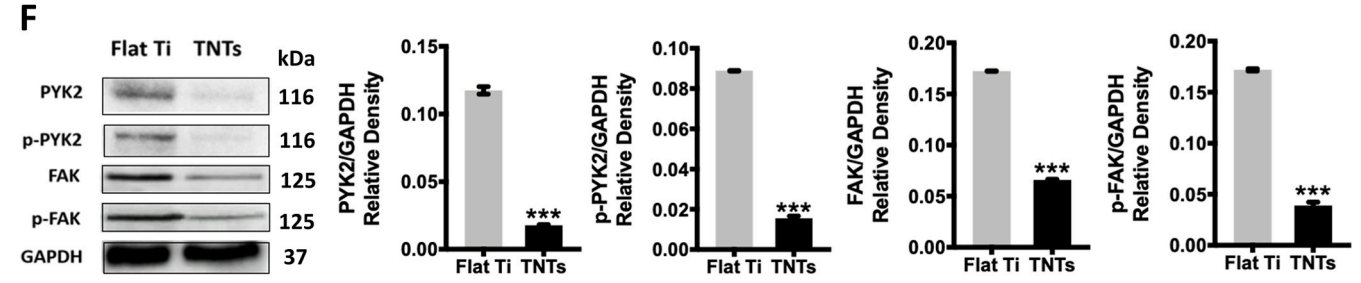

(caption on next page)

Fig. 1. Effects of titanium nanotopography on osteogenesis (A)The schematic shows that TNTs promote osteoblast differentiation and alter gene expression and osteogenic ability; (B) SEM images of the TNT morphologies and MC3T3-E1 attachments. SEM image of Flat Ti and TNTs (scale bars = 200 nm); (C) Detection of TNT-induced Osteogenesis: EDX spectra of the extracellular matrix on Flat Ti and a mineral deposit on TNTs after 21 days of culture; (D) Relative mRNA expression levels of the osteogenic markers Ocn, Runx2, Bsp and Osx expression in MC3T3-E1 cells on Flat Ti and TNT substrates; (E) Immunofluorescence staining of MC3T3-E1: F-actin staining (green), FAK or PYK2(red) and DAPI for nuclear staining (blue) on Flat Ti and TNTs (scale bars = 25 μm); (F) Western blot results and quantitative analysis of total FAK, total PYK2, FAK Y397 and PYK2 Y402 phosphorylation; All the values are presented as the means ± SDs. *$p < 0.05$, **$p < 0.01$, ***$p < 0.001$; $n = 3$. (For interpretation of the references to color in this figure legend, the reader is referred to the Web version of this article.)

surface of TNTs compared with those on Flat Ti (Fig. 2E), which was consistent with the previous results obtained with osteogenic precursor cells on nanotopography. Moreover, Western blotting revealed that the expression of total FAK, pY397-FAK, PYK2, and pY402-PYK2 was impaired by TNTs during the osteoclastic differentiation of BMMs on the surface of Flat Ti as well as on the surface of TNTs (Fig. 2F). These data suggest that compared with Flat Ti, TNTs inhibit the protein expression of FAK and PYK2 in BMM cells, inhibiting osteoclast formation.

3.3. Altering FAK and PYK2 expression levels differentially regulates osteogenesis

To investigate the effects of FAK and PYK2 on cellular osteogenic differentiation, lentivirus overexpression of FAK and PYK2 were successfully constructed. On polystyrene plate, FAK and PYK2 were silenced and overexpressed in MC3T3-E1 cells to observe the effects of the two proteins on osteogenic differentiation as shown in the schema (Fig. 3A). Western blotting revealed that lentivirus infection significantly increased FAK (Fig. S3A) and PYK2 (Fig. S3B) protein expression in MC3T3-E1 cells. Moreover, we constructed siRNAs to silence the expression of FAK and PYK2. FAK-knockdown (Fig. S5A) and PYK2-knockdown (Fig. S5B) cells were generated via Western blotting. After the treatment of MC3T3-E1 cells with small interfering RNA on polystyrene culture plates, an ALP staining assay (Fig. 3B) showed that the knockdown of PYK2 with small interfering RNA and coknockdown of PYK2 and FAK significantly enhanced osteogenic differentiation function compared to that of MC3T3-E1 cells treated with a nontargeted control. Overexpression of PYK2 and coexpression of PYK2 and FAK significantly impaired MC3T3-E1 cell osteogenic differentiation, which was consistent with the results of the alizarin red quantitative assay (Fig. 3D). Overall, ALP staining indicated that FAK and PYK2 coregulate the osteogenic differentiation capacity of MC3T3-E1 cells. Alizarin red staining and quantitative analysis of the results further revealed that the mineralization capacity of the dual-inhibited FAK/PYK2 group was significantly greater than that of the other groups after 14 days of culture (Fig. 3C). Next, we used real-time PCR to detect the effects of FAK and PYK2 on osteogenesis-related genes. We found FAK overexpression and FAK knockdown (Fig. 3E). The expression of only single bone marker genes was altered, and no significant differences between these two groups were observed. Notably, PYK2/FAK overexpression in MC3T3-E1 cells significantly suppressed osteogenic gene expression (Fig. 3F). In contrast, PYK2 overexpression and knockdown had critical effects on cell differentiation (Fig. 3E). As a result of PYK2 upregulation and downregulation, the osteogenic gene expression levels of MC3T3-E1 cells were significantly reduced and increased, respectively. Moreover, simultaneous knockdown of FAK and PYK2 significantly promoted osteogenic gene expression, which was the same effect as knockdown of PYK2 alone (Fig. 3E and F). The simultaneous overexpression of FAK and PYK2 also had a significant regulatory effect on the expression of Bsp, a gene related to late osteogenesis. Taken together, these data demonstrate that cellular osteogenic differentiation is increased by simultaneously inhibiting the expression level of PYK2.

3.4. Influence of the upregulation and downregulation of FAK and PYK2 on the osteoclast differentiation capacity of BMMs

To investigate the effects of FAK and PYK2 on cellular osteoclastic differentiation, we successfully established cellular FAK overexpression (Fig. S4A), PYK2 overexpression (Fig. S4B), FAK/PYK2 overexpression, FAK knockdown (Fig. S6A), PYK2 knockdown (Fig. S6B), and FAK/PYK2 knockdown models in mouse BMMs. On polystyrene plate, FAK and PYK2 were silenced and overexpressed in BMMs to observe the effects of the two proteins on osteoclastic differentiation as shown in the schema (Fig. 4A). When BMMs were treated with small interfering RNA on polystyrene culture plates and osteoclastic differentiation was induced, TRAP staining assays suggested that the knockdown of PYK with small interfering RNA and the coknockdown of PYK2 and FAK significantly inhibited osteoclasts formation compared with that in BMMs treated with the nontargeted control (Fig. 4B). Moreover, BMMs overexpressing FAK, PYK2, and FAK/PYK2 were successfully constructed and induced to differentiate into osteoclasts via lentivirus infection on polystyrene culture plates, and we found that PYK2 and FAK/PYK2 significantly inhibited osteoclasts formation compared with that upon the overexpression of FAK. Next, we used real-time PCR to detect the effects of FAK and PYK2 on osteoclastic

related genes (Fig. 4C and D). We found that the overexpression or knockdown of FAK (Fig. 4C and D) did not result in significant changes in osteoclastic related genes. In contrast, the overexpression and knockdown of PYK2 (Fig. 4C and D) had a critical effect on osteoclastic differentiation, the expression of PYK2 showed a positive correlation with the expression of osteoclastic genes, and the overexpression of both FAK and PYK2 and the knockdown of PYK2 had more significant effects on the expression of osteoclastic genes in osteoclastic cells. Taken together, these data demonstrate that osteoclastic differentiation was inhibited by simultaneously suppressing the expression of PYK2 and FAK. In contrast to FAK , the expression level of PYK2 on polystyrene fibers determines their osteoclastic differentiation ability.

3.5. Dual-mediated effects of PYK2 and FAK on bone homeostasis

Our data indicate that dual inhibition of PYK2 and FAK on polystyrene culture plates significantly promoted the osteogenic differentiation of cells and significantly inhibited the osteoclastic differentiation of cells. On the surface of TNTs, FAK and PYK2 were overexpressed on MC3T3-E1 and BMMs, and the effects of the two proteins on osteoblasts and osteoclasts were observed, as shown in schema (Fig. 5A). The expression of both FAK and PYK2 was downregulated on the surface of TNTs. Next, we utilized lentivirus to overexpress and coexpress FAK (Fig. S7A)and PYK2(Fig. S7B) on the surface of TNTs transformed with MC3T3-E1 and BMMs. Alizarin red staining revealed that the overexpression of FAK, the overexpression of PYK2, and the coexpression of FAK and PYK2 decreased the osteogenic differentiation of the cells in that order (Fig. 5B). The osteogenic ability of cells coexpressing these two genes was comparable to that of cells coexpressing PYK2. This findings was consistent with the trend observed by ALP staining (Fig. 5C). To investigate the important roles of FAK and PYK2 in osteogenesis, real-time PCR was performed, and the results showed that FAK overexpression did not significantly affect the expression of osteogenesis-related genes on TNTs, while PYK2 overexpression significantly inhibited the expression of osteogenesis-related genes (Fig. 5D). Western blotting revealed that the overexpression of PYK2 and the overexpression of FAK and PYK2 on TNTs significantly inhibited the expression of the osteogenic differentiation-related proteins OCN and OPN (Fig. 5E). Based on the previous results, we concluded that TNTs significantly inhibited the total protein and phosphorylation levels of FAK and PYK2. Therefore, we used inhibitors of FAK and PYK2 on

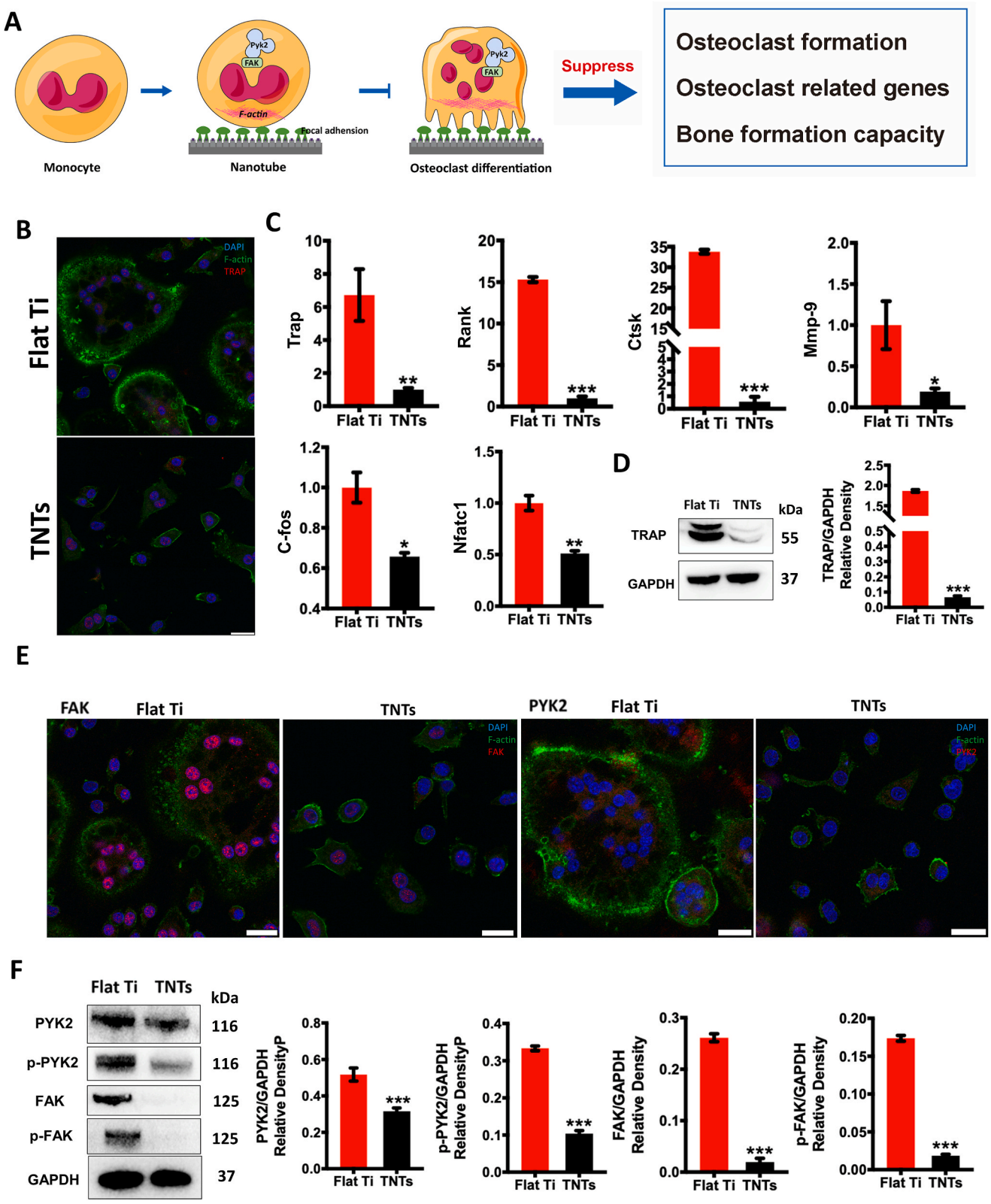

Fig. 2. Effects of titanium nanoporous topography on osteoclastogenesis (A) Schematic diagram showing that TNTs inhibited osteoclast differentiation, regulating osteoclast-related genes and thereby regulating bone formation. (B) Immunofluorescence staining of osteoclasts (TRAP [red], F-actin [green] and DAPI for nuclear staining [blue] on flat Ti and TNTs [scale bars = 25 μm]. (C) Relative mRNA expression levels of the osteoclastic markers Trap, Rank,Ctsk,Mmp-9,c-Fos and Nfatc1 expression in BMMs on Flat Ti and TNT substrates. (D) Western blot results and quantitative analysis of TRAP after inducing osteoclastic differentiation of BMMs with RANKL and M-CSF. (E) Immunofluorescence staining of osteoclasts (F-actin staining [green], FAK or PYK2 [red]) and DAPI for nuclear staining [blue] on flat Ti and TNTs [scale bars = 25 μm]. (F) Western blot results and quantitative analysis of total FAK, total PYK2, FAK Y397 and PYK2 Y402 phosphorylation. All the values are presented as the means ± SDs. *$p < 0.05$, **$p < 0.01$, ***$p < 0.001$; $n \geq 3$. (For interpretation of the references to color in this figure legend, the reader is referred to the Web version of this article.)

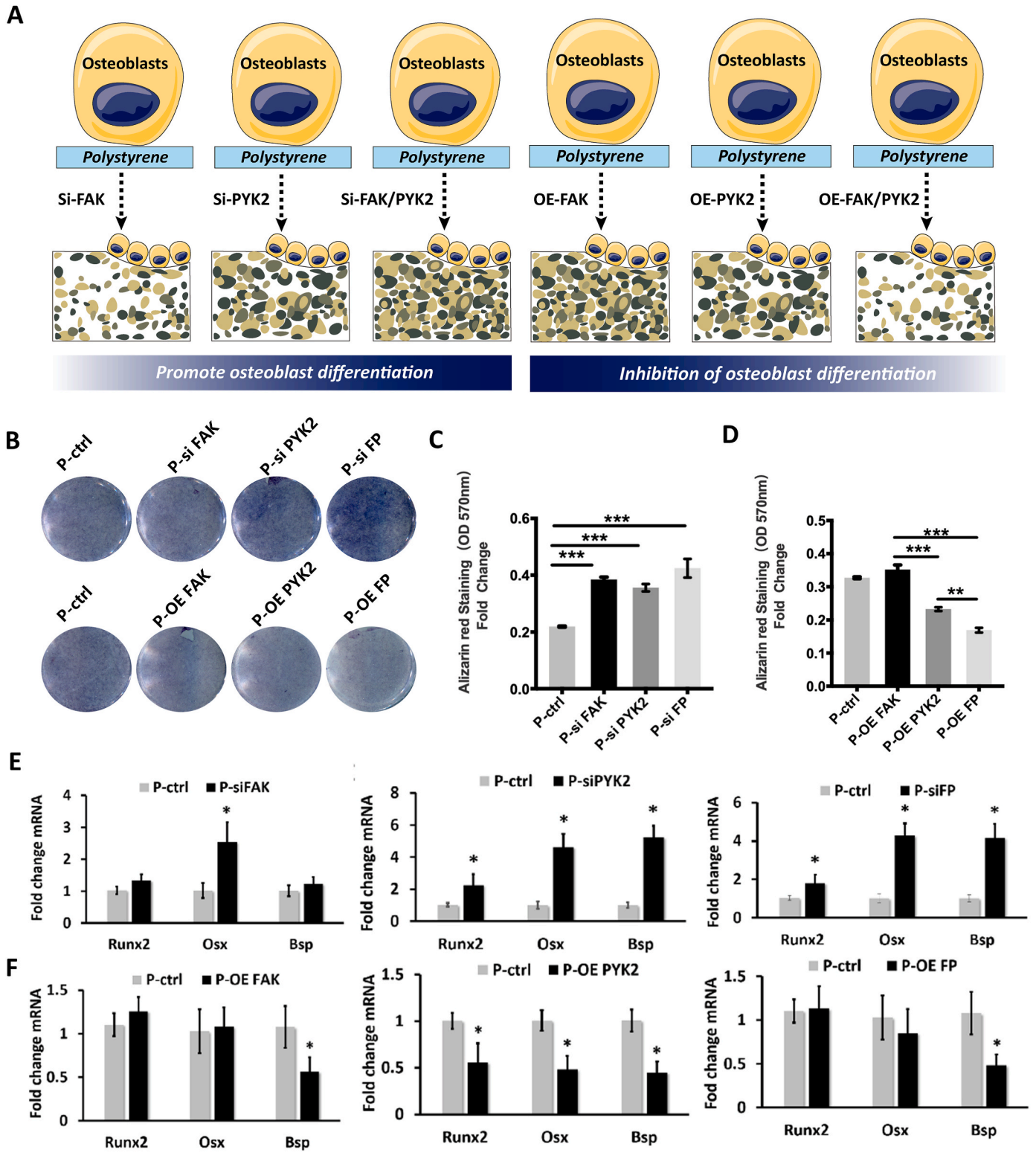

Fig. 3. The Effect of FAK and PYK2 regulate osteogenesis (A) Schematic showing the effects of both FAK and PYK2 inhibition and FAK and PYK2 overexpression on the osteoblastic differentiation of MC3T3-E1 cells. (B) Alkaline phosphatase staining after FAK and PYK2 knockdown or MC3T3-E1 overexpression for 7 days. MC3T3-E1 cells were treated with si-FAK, si-PYK2 and coknockdown FAK and PYK2 and were subsequently transfected with lentivirus for OE-FAK, OE-PYK2, or OE-FP on polystyrene culture plates. (C–D) Alizarin red staining of MC3T3-E1 cells with FAK/PYK2 knockdown and FAK/PYK2 overexpression for 14 days. (E) Relative mRNA expression levels of the osteogenic markers Ocn, Runx2, Bsp and Osx in MC3T3-E1 cells with FAK or PYK2 knockdown and coknockdown FAK/PYK2 on polystyrene culture plates. (F) Relative mRNA expression levels of the osteogenic markers Ocn, Runx2, Bsp and Osx in MC3T3-E1 cells overexpressing FAK or PYK2 and co-overexpressing FAK/PYK2 on polystyrene culture plates. All the values are the means ± SDs. *$p < 0.05$, **$p < 0.01$, ***$p < 0.001$, $n \geq 3$. (For interpretation of the references to color in this figure legend, the reader is referred to the Web version of this article.)

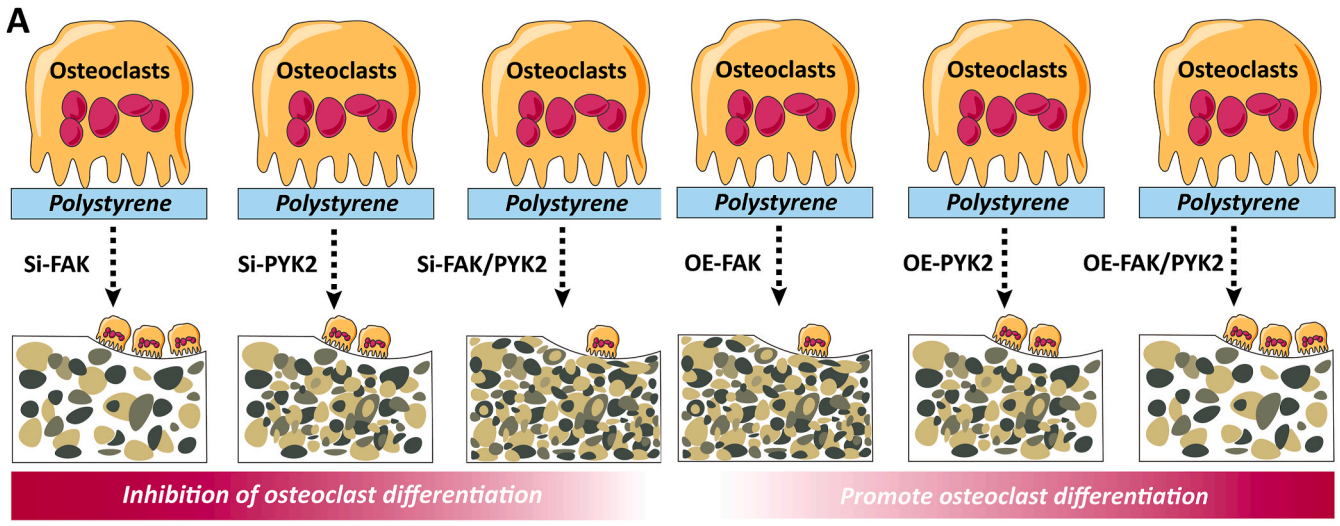

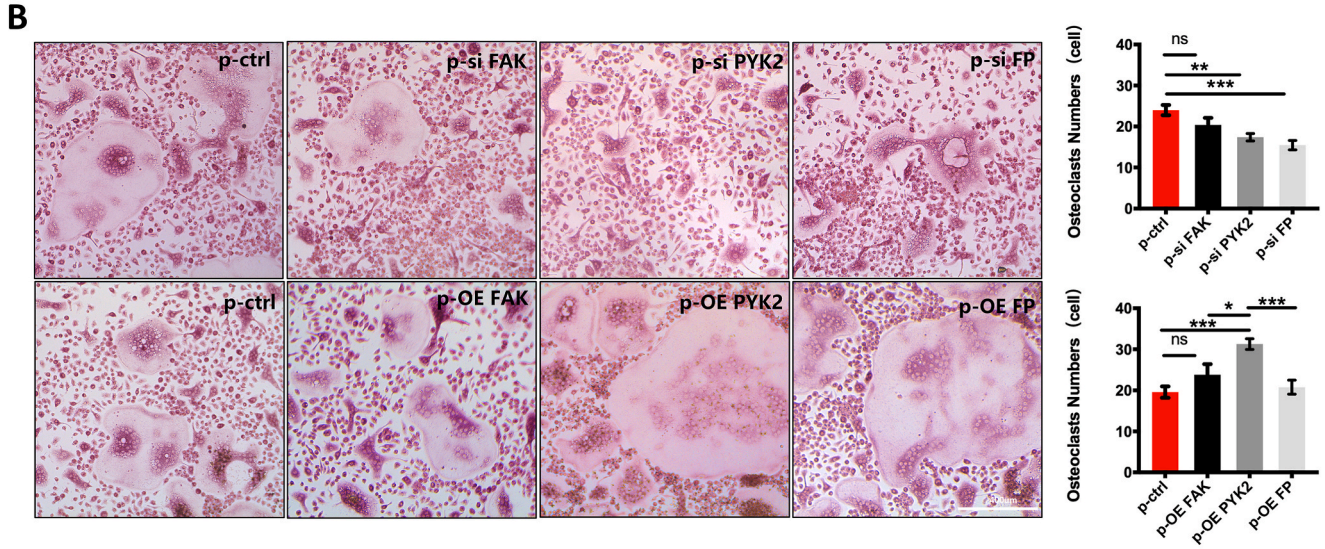

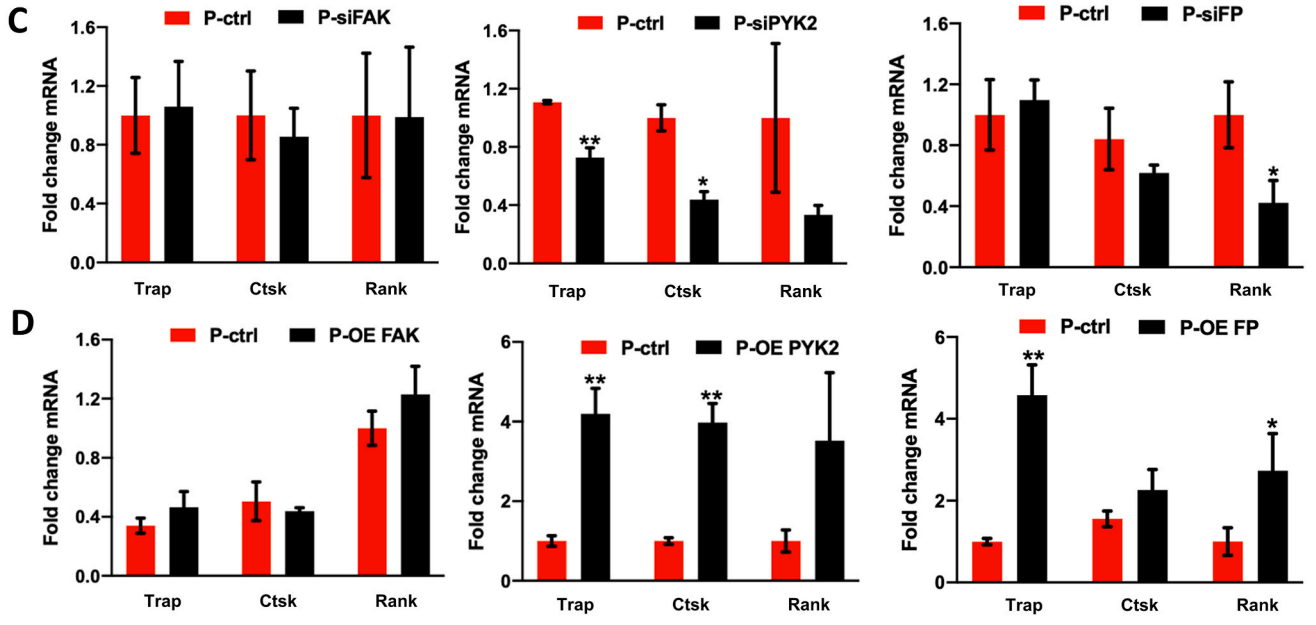

(caption on next page)

Fig. 4. The effect of FAK and PYK2 on osteoclastic differentiation (A) The schematic illustrates the effects of dual inhibition of FAK and PYK2 and overexpression of FAK and PYK2 on the osteoclastic differentiation of BMMs. (B) TRAP staining and osteoclast count. BMMs were subjected to RANKL and M-CSF for osteoclast differentiation for 4 days on polystyrene culture plates with FAK knockdown, PYK2 knockdown, FAK knockdown, PYK2 overexpression, PYK2 overexpression and FAK/PYK2 coexpression (scale bars = 400 μm). (C) Relative mRNA expression levels of the osteoclastic markers Trap, Rank, and Ctsk after FAK knockdown, PYK2 knockdown, and FAK/PYK2 coknockdown on polystyrene culture plates. (D) Relative mRNA expression levels of the osteoclastic markers Trap, Rank, and Ctsk in BMMs overexpressing FAK or PYK2 and co-overexpressing FAK/PYK2 on polystyrene culture plates. All the values are presented as the means ± SDs. *$p < 0.05$, **$p < 0.01$, ***$p < 0.001$, $n \geq 3$.

smooth titanium surfaces to observe osteogenesis. Western Blotting revealed that PF431396 significantly inhibited the phosphorylation levels of FAK (Fig. S8A) and PYK2 (Fig. S8B) at the concentration of 1uM without affecting the total protein level, so we chose to study at the concentration of 1uM. Next, MC3T3-E1 cells were implanted on Flat Ti plates and cultured for 7 or 14 days. Osteogenic ability was detected by alkaline phosphatase staining (Fig. S9A)and alizarin red staining (Fig. S9B). The results showed that the dual inhibition of FAK and PYK2 on flat Ti significantly improved bone formation ability. To further investigate the effects of FAK and PYK2 on osteoclast differentiation on the TNTs, we labeled osteoclasts by filamentous actin (F-actin) staining, and BMMs overexpressing PYK2 induced the production of more osteoclasts than those overexpressing FAK (Fig. 5F). Real-time PCR revealed that FAK overexpression had no significant effect on the expression of osteoclast-related genes on the TNT surfaces, while overexpression of PYK2 overexpression significantly promoted the expression of osteoclast-related genes (Fig. 5G). Western blotting revealed that compared with FAK overexpression, PYK2 overexpression significantly increased TRAP expression (Fig. 5H). Notably, both PCR and Western blotting showed that the two coexpressed genes most significantly improved the osteoclastic differentiation ability of BMMs. To further explore the different roles of FAK and PYK2 in inhibiting osteoclast differentiation on TNTs, we overexpressed FAK and PYK2 in BMMs and detected TRAP protein levels. Western blotting revealed that PYK2 played a significantly greater role than FAK in the process of osteoclast differentiation on TNTs (Fig. S10). Taken together, these data demonstrate that TNTs regulate the fate of osteoblasts and osteoclast differentiation through dual regulation of FAK and PYK2 expression levels.

3.6. TNTs mediate the ability of PYK2 but not FAK to regulate osteogenesis

To evaluate the effect of biophysical patterns on bone formation, the early osteoinductive capacity of different implant surfaces was dynamically assessed in vivo. Three-dimensional (3D) reconstructed microcomputed tomography (CT) scans were performed on days 3, 7, and 14 after implantation, and we observed that the surface of the TNTs had better osteogenic capacity(Fig. 6A). Micro-CT scans revealed better osseointegration of the TNTs, with the TNTs exhibiting a significant increase in the bone volume to trabecular volume (BV/TV), trabecular number (Tb.N), and trabecular thickness (Tb.Th) compared to those of the flat Ti group(Fig. 6B).Surprisingly, the positive expression of PYK2 (Fig. 6C) around the implant was significant, while the expression of FAK(Fig. 6D) was not obvious, suggesting that implant-promoted bone formation is highly correlated with PYK2. Immunohistochemical staining showed that OCN(Fig. 6E) and OPN (Fig. 6F)expression was significantly upregulated as early as day 7, suggesting that the nanostructured bone implants have a stronger osteoinductive ability. In addition, the distribution of osteoclasts around the implants was determined by TRAP staining(Fig. 6E), and on day 4, TRAP-positive osteoclasts were clearly visible near the surface of the implants(Fig. 6F), and the number of osteoclasts on the TNT implants was less than that on the Flat Ti implants. In summary, nanotopological structured implants promoted osteoblast differentiation, and inhibited osteoclast formation associated with PYK2.

4. Discussion

In this study, nanotubular porous structures were used as a model for the regulation of cell fate by mechanical stimulation, on the basis of which the specific functions of FAK and PYK2 were demonstrated. We found that TNT nanomorphology plays a significant role in promoting osteogenic differentiation and inhibiting osteolytic differentiation. FAK and PYK2 are both important transmitters of adhesion-related signals and structurally homologous, but their functional specificity in regulating cell fate in response to mechanical stimulation is unclear. Through this study, we found that the following: 1. The total protein expression and phosphorylated protein levels of FAK and PYK2 were significantly inhibited on the titanium nanotube torphological surface, promoting osteogenesis and inhibiting osteoclast. 2. When siRNAs to silence the expression levels of FAK and PYK2 in mouse precursor MC3T3-E1 cells were constructed, silencing the expression of FAK had no significant effect on cells. Furthermore, silencing FAK had no significant effect on osteogenic differentiation, but the co-silencing of PYK2 and FAK significantly promoted osteogenic differentiation and the expression of related genes. 3. We found that the downregulation of FAK tended to inhibit osteogenic differentiation, but the effect was still not significant; however, silencing PYK2 and the co-silencing of PYK2 and FAK significantly inhibited the osteoclastic differentiation of cells. 4. FAK was expressed at low levels in cells, while FAK expression was less pronounced.

Cell adhesion is the key to determining the fate of differentiation in response to biomechanical signals [29]. The adhesion plaque is a starting point in response to external changes, and the adhesion kinase family includes two homologous members, proline-rich tyrosine kinase 2 (FAK) and proline-rich tyrosine kinase 2 (PYK2), which are primarily known as regulators of cytoskeletal dynamics and cell adhesion in nucleated cells [27]. FAK acts primarily as a traditional focal adhesion kinase activated downstream of integrin, while PYK2 coordinates multiple signals from different receptors [30]. FAK and PYK2, key proteins in extracellular signaling, play important roles in regulating cell differentiation [26]. The surface shape of ideal bone implants can better promote the differentiation of osteoblasts and inhibit the function of osteoclasts to achieve a more stable effect. Our previous studies showed that the osteogenic differentiation level of mouse MC3T3-E1 precursor cells is significantly changed, while osteoclastic activity is not affected [15]. Previous studies have shown that extensive bone destruction (osteolysis) by osteoclasts is the cause of peri-implant loosening. The effect of bone implants on osteoclast differentiation, fusion and other physiological processes is worthy of attention [31]. Consistent with previous studies, osteoclast formation was significantly inhibited on the surface of TNTs [32]. As highlighted by our observations, both FAK and PYK2 expression and phosphorylation were inhibited on the surface of TNTs, which suggests that the osteogenic differentiation of cells induced by the morphological structure of TNTs does not depend on a downstream cascade response induced by FAK and PYK2 activation. In contrast to previous studies, focal adhesion kinase (FAK) mechanically affects osteoblast maturation and its own expression is not significantly affected [33]. PYK2 plays a significant role in inhibiting osteogenesis in response to mechanical adhesion signals [34]. The question is whether FAK and PYK2 play unique roles in the nanomorphogenic promotion of bone formation.

FAK is an important tyrosine kinase that transduces key signals from FAs to regulate a variety of cellular activities, including survival,

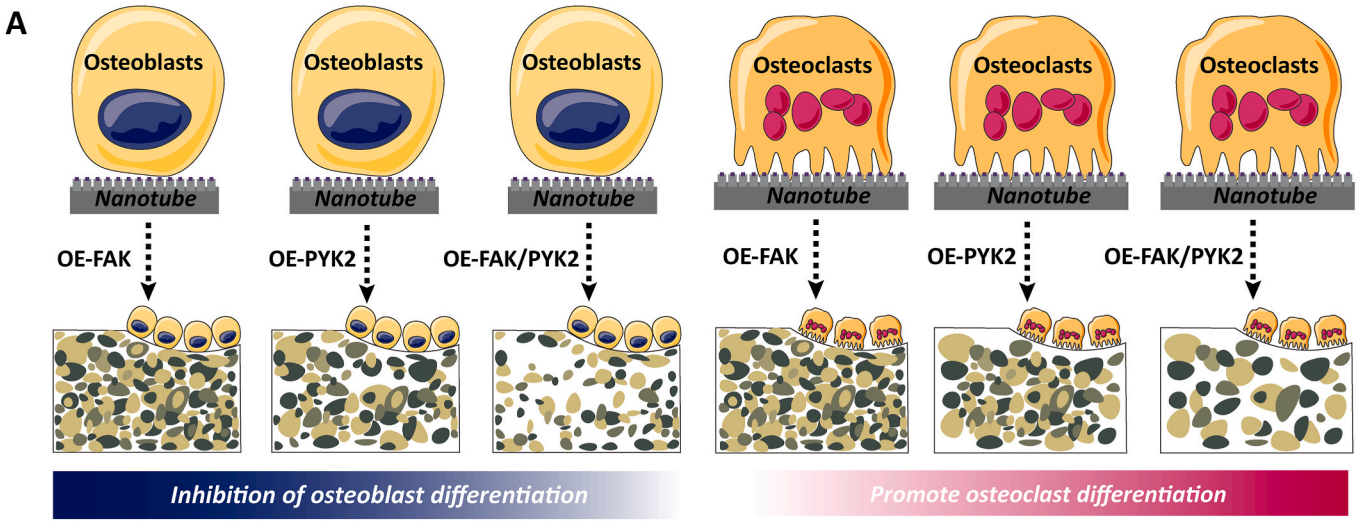

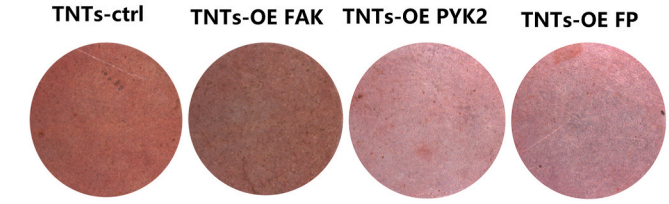

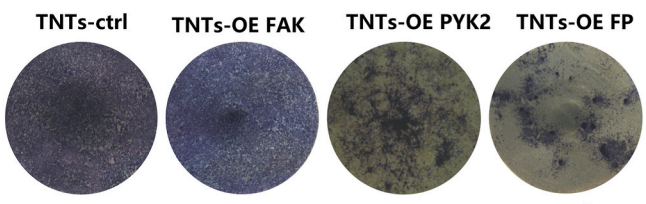

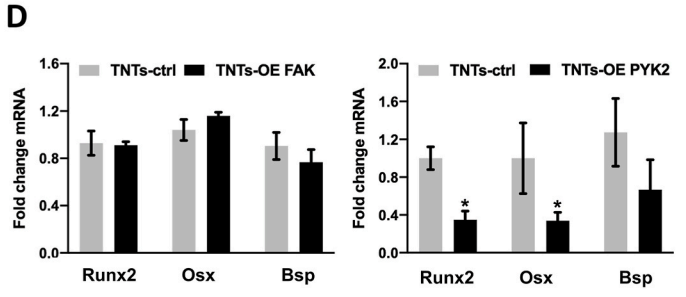

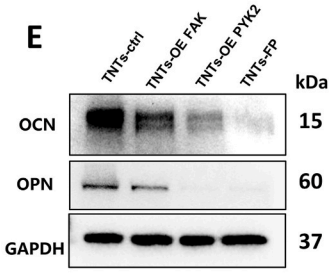

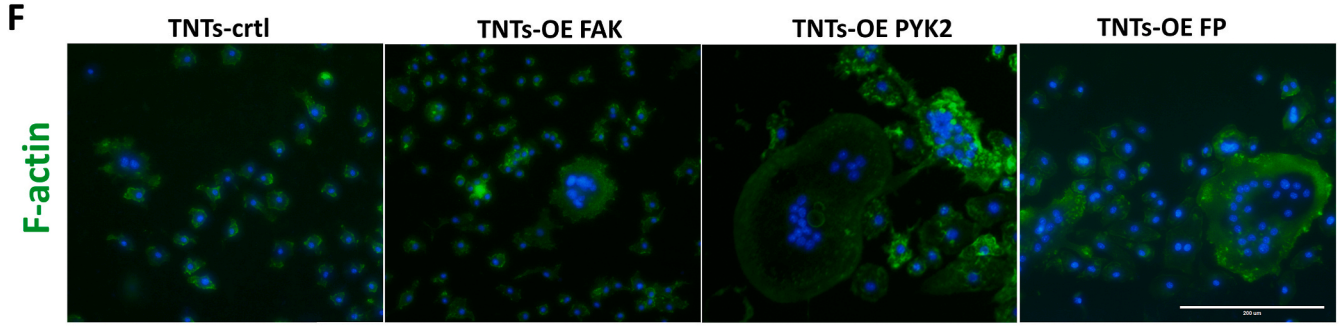

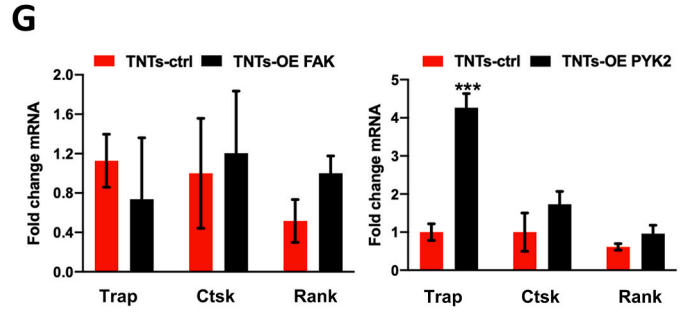

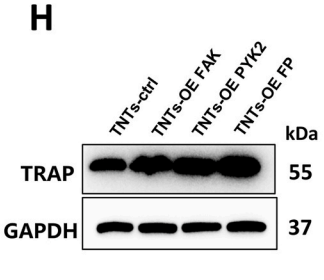

(caption on next page)

Fig. 5. Effect of PYK2 or FAK overexpression on TNT-mediated regulation of osteoblastic and osteoclastic differentiation (A) The schematic illustrates the effects of double overexpression of FAK and PYK2 on the balance of osteoblasts and osteoclasts on the TNT surface. (B) Alizarin red staining of MC3T3-E1 cells for 14 days after overexpressing FAK or PYK2 and co-overexpressing FAK/PYK2 on the TNTs. (C) ALP staining of MC3T3-E1 cells for 7 days after overexpressing FAK or PYK2 and co-overexpressing FAK/PYK2 on the TNTs. (D) Relative mRNA expression levels of the osteogenic markers Runx2, Bsp and Osx in MC3T3-E1 cells overexpressing FAK and PYK2 on the TNTs. (E) Western blot results showing FAK or PYK2 overexpression and co-overexpressing FAK/PYK2 on the protein levels of OCN and OPN. (F) Phalloidin staining of the osteoclast cytoskeleton. F-actin (green) and DAPI for nuclear staining (blue) on TNTs (scale bars = 25 μm). (G) Relative mRNA expression levels of the osteoclastic markers Trap, Rank and Ctsk in BMMs overexpressing FAK or PYK2 and co-overexpressing FAK/PYK2 on TNTs. (H) Western blot results showing FAK or PYK2 overexpression and FAK/PYK2 co-overexpression on the protein level of TRAP. All the values are the means ± SDs. *$p < 0.05$, **$p < 0.01$, ***$p < 0.001$, $n \geq 3$. (For interpretation of the references to color in this figure legend, the reader is referred to the Web version of this article.)

migration, and mechanical sensing [30,35].FAK has been widely recognized to play an active role in bone differentiation in response to mechanical stimulation [36].PYK2 as the non-receptor tyrosine kinase has several features of FAK [37], including the recruitment of Src-family kinases after autophosphorylation and the activation of downstream mechanical signaling pathways [25]; however, recent studies have suggested PYK2 may also contribute to bone formation [38]. In the present study, TNTs were shown to successfully alter osteogenesis and osteoclastogenesis while downregulating the expression of FAK and PYK2 and their active phosphorylated forms.

Therefore, to elucidate the roles of FAK and PYK2 in osteogenic/osteoblastic differentiation, we regulated FAK and PYK2 gene expression via siRNA knockdown and lentivirus overexpression. In the absence of nanomorphic stimulation, the overexpression of FAK did not significantly alter the expression levels of genes related to osteogenic/osteoclast differentiation, whereas the overexpression of PYK2 inhibited the expression of osteogenic genes and promoted the expression of osteoclast genes. However, interestingly, the effects of co-overexpression of PYK2 and FAK were consistent with PYK2 overexpression. Notably, compared to silencing FAK, silencing PYK2 significantly promoted osteogenic differentiation to a level that inhibited the expression of osteoblast-related genes, suggesting that the inhibition of PYK2 alone promotes cellular osteogenic differentiation, providing a new method for determining cell fate. Additionally, even though FAK silencing had no significant effect on the levels of osteogenic/osteoclastogenic genes, the cosilencing of FAK and PYK2 very significantly promoted bone formation and suppressed the expression of osteoclastogenic genes. Further studies suggested that the bidirectional inhibition or enhancement of PYK2/FAK expression is more effective in regulating osteogenic and osteoblastic homeostasis.

In view of the active roles of FAK [39] and PYK2 in the process of bone homeostasis maintenance by both osteogenesis and osteoclasts [33], this study showed that the inhibition of FAK and PYK2 expression can promote osteoblast differentiation and inhibit osteoclast differentiation to further explain the specific functions of FAK and PYK2 in regulating mechanical transmission [20]. In this study, after the infection of BMMs with lentivirus expressing FAK and siRNA silencing of FAK expression in BMMs, we found that altering FAK gene expression under TNT stimulation had little effect on osteoclast differentiation. PYK2, a cytoplasmic adhesion kinase associated with FAK, has been shown to positively regulate osteoclast formation. Loss of PYK2 in vivo improves osteogenesis and may be a negative regulator of osteogenesis [2]. However, it is worth noting that bone formation is a dynamic balance process involving both osteoblasts and osteoclasts. This study involved a series of mechanisms to initiate functional differentiation through cell adhesion and surface morphology based on the surface morphology of titanium nanoparticles. We elucidate the morphology-dependent osteogenic and osteoclastic responses at gene level and protein level respectively. Consistent with the results of the present study, the level of PYK2 expression in osteoblasts more likely affected the gene expression and activity of osteoclasts than FAK expression. Subsequent in vivo experiments further confirmed that the distribution and number of PYK2+ cells around the implant were significantly increased, suggesting that PYK2 plays a key role in promoting bone formation via TNTs. Notably, a nanomorphic surface with bidirectional knockdown of the PYK2 and FAK genes in BMMs almost completely inhibited osteoclast formation. However, our limited data could not demonstrate whether the phosphorylation levels of FAK and PYK2 are related to cell differentiation, and the detailed mechanism by which PYK2 and FAK regulate TNT-induced cellular osteogenic/osteoclastic differentiation needs to be further investigated. In addition, it is worth noting that there are still many factors involved in the process of bone integration mediated by mechanical stimulation, including intramembrane osteogenesis and intrachondral osteogenesis. The specific mechanism of exploring the surface topography characteristics of bone tissue biomaterials in multiple dimensions lays a foundation for the precise regulation of bone homeostasis around implants [40].

In summary, we systematically compared the unique functions of two members of the adherent spot kinase family, FAK and PYK2, in regulating osteogenic-osteolytic differentiation on a nanomorphic surface. Our findings suggest that differences in PYK2 expression induced by a nanomorphic surface have a key effect on the morphology of newly formed bone. Consistent with these findings, PYK2 had a much greater effect on cellular osteogenic differentiation than FAK did on osteogenesis, even in the absence of nanomorphic stimulation. Notably, both PYK2 and FAK double knockdown and overexpression further enhanced the differences in cellular phenotypes compared to the effects of PYK2 alone as well as FAK, and we wondered whether these two kinases exert functional redundancy. An in-depth study of the detailed mechanisms of FAK and PYK2 in driving cellular behaviors by mechanical stimulation has established new targets for optimizing the surface structure of Ti implants to improve osseointegration.

Statistical analysis

All the results are expressed as the mean ± standard deviation. Differences between two groups were evaluated with an unpaired Student's *t*-test. Statistical analysis of differences among three or more groups was evaluated with one-way analysis of variance. $p < 0.05$ was considered to indicate statistical significance. GraphPad Prism 8 (GraphPad, USA) software was used for all the statistical analyses and graphical representations.

CRediT authorship contribution statement

Tao Chen: Writing – original draft, Methodology, Data curation. **MingXing Ren:** Investigation. **YuZhou Li:** Software, Resources. **Zheng Jing:** Software, Investigation. **XinXin Xu:** Validation, Formal analysis. **FengYi Liu:** Project administration, Formal analysis. **DingQiang Mo:** Methodology. **WenXue Zhang:** Supervision. **Jie Zeng:** Software. **He Zhang:** Writing – original draft, Methodology, Funding acquisition. **Ping Ji:** Writing – review & editing, Supervision. **Sheng Yang:** Writing – review & editing, Funding acquisition, Conceptualization.

Declaration of competing interest

The authors declare that they have no known competing financial interests or personal relationships that could have appeared to influence the work reported in this paper.

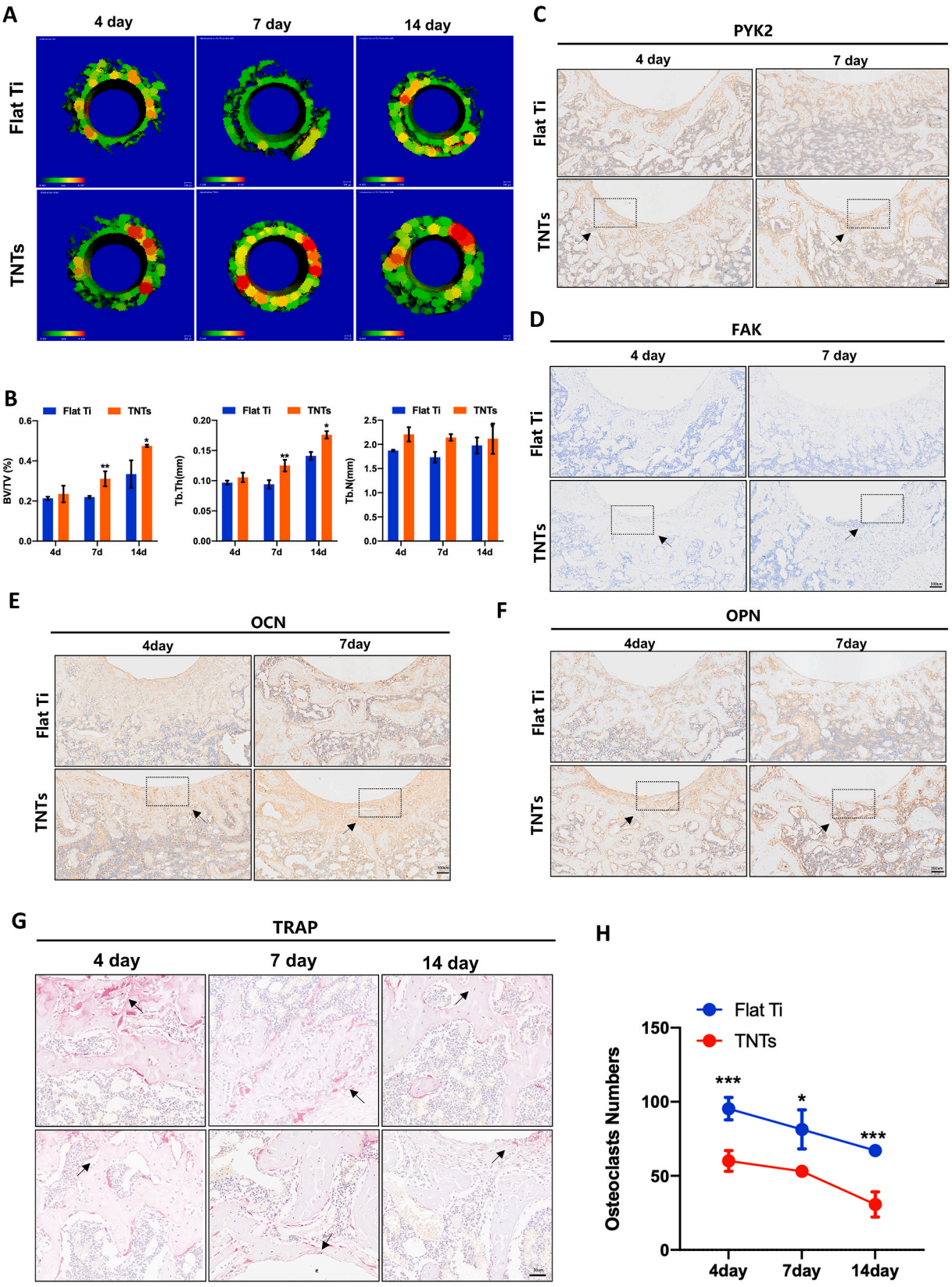

Fig. 6. TNTs regulation of osteogenesis is related to PYK2 (A) 3D reconstruction of micro-CT data depicting new bone formation; (B) Quantification of BV/TV, TbN, and TbTh and in the ROI of micro-CT data for 4 and 7 days after implantation; (C–F) Immunohistochemical staining of PYK2, FAK, OCN and OPN indicating bone regeneration on the implant surface (scale bars = 100 μm); (G) Peri-implant TRAP staining at 4, 7, and 14 days after implantation (scale bars = 50 μm); (H) Accounts of TRAP-positive cells at 4, 7, and 14 days after implantation. All the values are the means ± SDs. *$p < 0.05$, **$p < 0.01$, ***$p < 0.001$, $n \geq 3$.

Data availability

Data will be made available on request.

Acknowledgments

This work was supported by the National Natural Science Foundation of China (Grant Nos. U23A20447, 82220108019, 82171010, 82170936, and 82371018), the Natural Science Foundation of Chongqing (Grant No. cstc2021jcyj-jqX0028 CSTB2022NSCQ-MSX0098) , the Scientific and Technological Research Program of Chongqing Municipal Education Commission (Grant No. KJQN202200422),the Program for Youth Innovation in Future Medicine, Chongqing Medical University (No. W0079), the Project of Chongqing Medical University Graduate Tutor Team (cqmudstd202203),and the Chongqing Scientific Research and Innovation Project for Postgraduates (Grant No. CYB22216).

Appendix A. Supplementary data

Supplementary data to this article can be found online at https://doi.org/10.1016/j.mtbio.2024.101038.

References

[1] M. Ortiz-Catalan, E. Mastinu, P. Sassu, O. Aszmann, R. Brånemark, Self-contained neuromusculoskeletal arm prostheses, N. Engl. J. Med. 382 (18) (2020) 1732–1738.
[2] L. Buckbinder, D. Crawford, H. Qi, H. Ke, L. Olson, K. Long, P. Bonnette, A. Baumann, J. Hambor, W. Grasser, L. Pan, T. Owen, M. Luzzio, C. Hulford, D. Gebhard, V. Paralkar, H. Simmons, J. Kath, W. Roberts, S. Smock, A. Guzman-Perez, T. Brown, M. Li, Proline-rich tyrosine kinase 2 regulates osteoprogenitor cells and bone formation, and offers an anabolic treatment approach for osteoporosis, Proc. Natl. Acad. Sci. U.S.A. 104 (25) (2007) 10619–10624.
[3] Y. Li, C. Chen, T. Trinh-Minh, H. Zhu, A. Matei, A. Györfi, F. Kuwert, P. Hubel, X. Ding, C. Manh, X. Xu, C. Liebel, V. Fedorchenko, R. Liang, K. Huang, J. Pfannstiel, M. Huang, N. Lin, A. Ramming, G. Schett, J. Distler, Dynamic changes in O-GlcNAcylation regulate osteoclast differentiation and bone loss via nucleoporin 153, Bone research 10 (1) (2022) 51.
[4] M. Tsukasaki, H. Takayanagi, Osteoimmunology: evolving concepts in bone-immune interactions in health and disease, Nat. Rev. Immunol. 19 (10) (2019) 626–642.
[5] L. Wang, X. You, L. Zhang, C. Zhang, W. Zou, Mechanical regulation of bone remodeling, Bone research 10 (1) (2022) 16.
[6] Y. Ren, J. Weeks, T. Xue, J. Rainbolt, K. de Mesy Bentley, Y. Shu, Y. Liu, E. Masters, P. Cherian, C. McKenna, J. Neighbors, F. Ebetino, E. Schwarz, S. Sun, C. Xie, Evidence of bisphosphonate-conjugated sitafloxacin eradication of established methicillin-resistant S. aureus infection with osseointegration in murine models of implant-associated osteomyelitis, Bone research 11 (1) (2023) 51.
[7] M. Rahmati, E. Silva, J. Reseland, C. A Heyward, H. Haugen, Biological responses to physicochemical properties of biomaterial surface, Chem. Soc. Rev. 49 (15) (2020) 5178–5224.
[8] C. Gu, Q. Zhou, X. Hu, X. Ge, M. Hou, W. Wang, H. Liu, Q. Shi, Y. Xu, X. Zhu, H. Yang, X. Chen, T. Liu, F. He, Melatonin rescues the mitochondrial function of bone marrow-derived mesenchymal stem cells and improves the repair of osteoporotic bone defect in ovariectomized rats, J. Pineal Res. (2023) e12924.
[9] J. Compston, M. McClung, W. Leslie, Osteoporosis, Lancet (London, England) 393 (10169) (2019) 364–376.
[10] Y. Tang, K. Wang, B. Wu, K. Yao, S. Feng, X. Zhou, L. Xiang, Photoelectrons sequentially regulate antibacterial activity and osseointegration of titanium implants, Adv. Mater. (2023) e2307756 (Deerfield Beach, Fla.
[11] X. Li, X. Luo, Y. He, K. Xu, Y. Ding, P. Gao, B. Tao, M. Li, M. Tan, S. Liu, P. Liu, K. Cai, Micronano titanium accelerates mesenchymal stem cells aging through the activation of senescence-associated secretory phenotype, ACS Nano 17 (22) (2023) 22885–22900.
[12] X. Li, J. Combs, K. Salaita, X. Shu, Polarized focal adhesion kinase activity within a focal adhesion during cell migration, Nat. Chem. Biol. 19 (12) (2023) 1458–1468.
[13] B. Xing, Z. Lei, Z. Wang, Q. Wang, Q. Jiang, Z. Zhang, X. Liu, Y. Qi, S. Li, X. Guo, Y. Liu, X. Li, K. Shu, H. Zhang, J. Bartsch, C. Nimsky, Y. Huang, T. Lei, ADAM22 activates integrin β1 through its disintegrin domain to promote the progression of pituitary adenoma, Neuro Oncol. (2023).
[14] L. Yu, Y. Hou, W. Xie, J. Cuellar-Camacho, Q. Wei, R. Haag, Self-strengthening adhesive force promotes cell mechanotransduction, Advanced materials (Deerfield Beach, Fla.) 32 (52) (2020) e2006986.
[15] H. Zhang, L.F. Cooper, X. Zhang, Y. Zhang, F. Deng, J. Song, S. Yang, Titanium nanotubes induce osteogenic differentiation through the FAK/RhoA/YAP cascade, RSC Adv. 6 (50) (2016) 44062–44069.
[16] Y. Fu, Z. Jing, T. Chen, X. Xu, X. Wang, M. Ren, Y. Wu, T. Wu, Y. Li, H. Zhang, P. Ji, S. Yang, Nanotube patterning reduces macrophage inflammatory response via nuclear mechanotransduction, J. Nanobiotechnol. 21 (1) (2023) 229.
[17] S. Shirazi, S. Ravindran, L. Cooper, Topography-mediated immunomodulation in osseointegration; ally or enemy, Biomaterials 291 (2022) 121903.
[18] I. Cockerill, Y. Su, J. Lee, D. Berman, M. Young, Y. Zheng, D. Zhu, Micro-/Nanotopography on bioresorbable zinc dictates cytocompatibility, bone cell differentiation, and macrophage polarization, Nano Lett. 20 (6) (2020) 4594–4602.
[19] Y. Yang, S. Li, Y. Wang, Y. Zhao, Q. Li, Protein tyrosine kinase inhibitor resistance in malignant tumors: molecular mechanisms and future perspective, Signal Transduct. Targeted Ther. 7 (1) (2022) 329.
[20] R. Ransom, A. Carter, A. Salhotra, T. Leavitt, O. Marecic, M. Murphy, M. Lopez, Y. Wei, C. Marshall, E. Shen, R. Jones, A. Sharir, O. Klein, C. Chan, D. Wan, H. Chang, M. Longaker, Mechanoresponsive stem cells acquire neural crest fate in jaw regeneration, Nature 563 (7732) (2018) 514–521.
[21] M. de Rooij, Y. Thus, N. Swier, R. Beijersbergen, S. Pals, M. Spaargaren, A loss-of-adhesion CRISPR-Cas9 screening platform to identify cell adhesion-regulatory proteins and signaling pathways, Nat. Commun. 13 (1) (2022) 2136.
[22] S. Min, H. Kang, S. Jung, D. Jang, B. Min, A vitronectin-derived peptide reverses ovariectomy-induced bone loss via regulation of osteoblast and osteoclast differentiation, Cell Death Differ. 25 (2) (2018) 268–281.
[23] P. Han, J. Frith, G. Gomez, A. Yap, G. O'Neill, J. Cooper-White, Five piconewtons: the difference between osteogenic and adipogenic fate choice in human mesenchymal stem cells, ACS Nano 13 (10) (2019) 11129–11143.
[24] B. Chang, C. Ma, X. Liu, Nanofibers regulate single bone marrow stem cell osteogenesis via FAK/RhoA/YAP1 pathway, ACS Appl. Mater. Interfaces 10 (39) (2018) 33022–33031.
[25] H. Gil-Henn, J. Girault, S. Lev, PYK2, a hub of signaling networks in breast cancer progression, Trends Cell Biol. (2023).
[26] S. Qi, X. Sun, H. Choi, J. Yao, L. Wang, G. Wu, Y. He, J. Pan, J. Guan, F. Liu, FAK promotes early osteoprogenitor cell proliferation by enhancing mTORC1 signaling, J. Bone Miner. Res. : the official journal of the American Society for Bone and Mineral Research 35 (9) (2020) 1798–1811.
[27] J. Lee, I. Lee, T. Iimura, S. Kong, Two macrophages, osteoclasts and microglia: from development to pleiotropy, Bone research 9 (1) (2021) 11.
[28] K. Curtis, T. Coughlin, D. Mason, J. Boerckel, G. Niebur, Bone marrow mechanotransduction in porcine explants alters kinase activation and enhances trabecular bone formation in the absence of osteocyte signaling, Bone 107 (2018) 78–87.
[29] S. Chen, T. He, Y. Zhong, M. Chen, Q. Yao, D. Chen, Z. Shao, G. Xiao, Roles of focal adhesion proteins in skeleton and diseases, Acta Pharm. Sin. B 13 (3) (2023) 998–1013.
[30] E. Kleinschmidt, D. Schlaepfer, Focal adhesion kinase signaling in unexpected places, Curr. Opin. Cell Biol. 45 (2017) 24–30.
[31] A. Qin, T.S. Cheng, Z. Lin, L. Cao, S.M. Chim, N.J. Pavlos, J. Xu, M.H. Zheng, K. R. Dai, Prevention of wear particle-induced osteolysis by a novel V-ATPase inhibitor saliphenylhalamide through inhibition of osteoclast bone resorption, PLoS One 7 (4) (2012) e34132.
[32] Y. He, Z. Li, X. Ding, B. Xu, J. Wang, Y. Li, F. Chen, F. Meng, W. Song, Y. Zhang, Nanoporous titanium implant surface promotes osteogenesis by suppressing osteoclastogenesis via integrin β1/FAKpY397/MAPK pathway, Bioact. Mater. 8 (2022) 109–123.
[33] C. Zheng, H. Liu, P. Zhao, W. Lu, S. Song, T. He, J. Fan, D. Wang, P. Yang, Q. Jie, H. Zheng, Z. Luo, L. Yang, Targeting sulfation-dependent mechanoreciprocity between matrix and osteoblasts to mitigate bone loss, Sci. Transl. Med. 15 (710) (2023) eadg3983.
[34] K. Bashour, A. Gondarenko, H. Chen, K. Shen, X. Liu, M. Huse, J. Hone, L. Kam, CD28 and CD3 have complementary roles in T-cell traction forces, Proc. Natl. Acad. Sci. U.S.A. 111 (6) (2014) 2241–2246.
[35] P. Prasad, A. Billah Khair, K. Venkatesan, M. Shahwan, A. Shamsi, Molecular and functional insight into focal adhesion kinases: therapeutic implications for oral malignancies, Drug Discov. Today (2023) 103852.
[36] C. Pagani, A. Bancroft, R. Tower, N. Livingston, Y. Sun, J. Hong, R. Kent, A. Strong, J. Nunez, J. Medrano, N. Patel, B. Nanes, K. Dean, Z. Li, C. Ge, B. Baker, A. James, S. Weiss, R. Franceschi, B. Levi, Discoidin domain receptor 2 regulates aberrant mesenchymal lineage cell fate and matrix organization, Sci. Adv. 8 (51) (2022) eabq6152.
[37] M. Franco, L. Tamagnone, Tyrosine phosphorylation in semaphorin signalling: shifting into overdrive, EMBO Rep. 9 (9) (2008) 865–871.
[38] L. Zhong, D. Liao, J. Li, W. Liu, J. Wang, C. Zeng, X. Wang, Z. Cao, R. Zhang, M. Li, K. Jiang, Y. Zeng, J. Sui, T. Kang, Rab22a-NeoF1 fusion protein promotes osteosarcoma lung metastasis through its secretion into exosomes, Signal Transduct. Targeted Ther. 6 (1) (2021) 59.
[39] Y. Huang, J. Liao, R. Vlashi, G. Chen, Focal adhesion kinase (FAK): its structure, characteristics, and signaling in skeletal system, Cell. Signal. 111 (2023) 110852.
[40] S. Ghimire, S. Miramini, G. Edwards, R. Rotne, J. Xu, P. Ebeling, L. Zhang, The investigation of bone fracture healing under intramembranous and endochondral ossification, BoneKEy Rep. 14 (2021) 100740.